

Received 21 November 2022
Accepted 10 January 2023

Edited by M. Zeller, Purdue University, USA

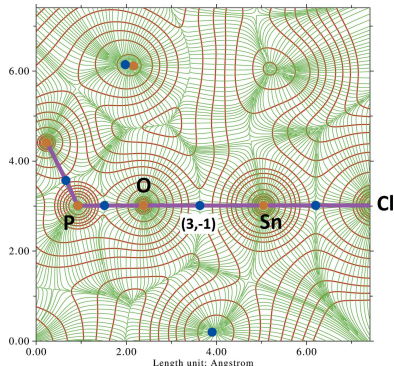
‡ Other affiliation: Laboratoire de Chimie Minérale et Analytique (LACHIMIA), Département de Chimie, Faculté des Sciences et Techniques, Université Cheikh Anta Diop, Dakar, Senegal.

This article is part of a collection of articles to commemorate the founding of the African Crystallographic Association and the 75th anniversary of the IUCr.

Keywords: crystal structure; stannane; triphenylphosphate; QTAIM; topology analysis.

CCDC reference: 2235598

Supporting information: this article has supporting information at journals.iucr.org/e



OPEN ACCESS

Published under a CC BY 4.0 licence

Synthesis and topology analysis of chloridotriphenyl(triphenyl phosphate- κ O)tin(IV)

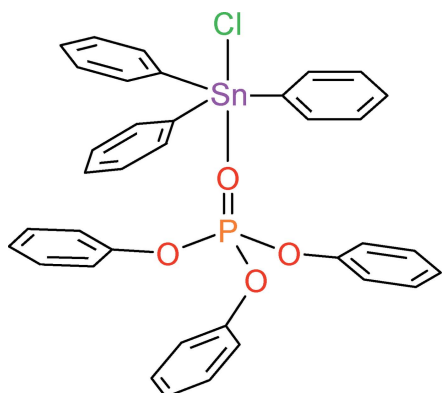
Serigne Fallou Pouye,^{a,*‡} Sylvain Bernès,^{b,*} Lamine Yaffa,^c Waly Diallo,^c Ibrahima Cissé,^{a‡} Cheikh Abdoul Khadir Diop,^c Mamadou Sidibé^c and Libasse Diop^c

^aDépartement de Sciences Appliquées et Technologies Emergentes, Ecole Supérieure des Sciences et Techniques de l'Ingénieur, Université Amadou Mahtar Mbow, BP 45927 Dakar NAFA VDN, Dakar, Senegal, ^bInstituto de Física, Benemérita Universidad Autónoma de Puebla, Av. San Claudio y 18 Sur, 72570 Puebla, Pue., Mexico, and ^cLaboratoire de Chimie Minérale et Analytique (LACHIMIA), Département de Chimie, Faculté des Sciences et Techniques, Université Cheikh Anta Diop, Dakar, Senegal. *Correspondence e-mail: serigne.pouye@uam.edu.sn, sylvain_bernes@hotmail.com

The title Sn^{IV} complex, $[\text{Sn}(\text{C}_6\text{H}_5)_3\text{Cl}(\text{C}_{18}\text{H}_{15}\text{O}_4\text{P})]$, is a formal adduct between triphenyl phosphate ($(\text{PhO})_3\text{P}=\text{O}$) and the stannane derivative chloridotriphenyltin, SnPh_3Cl . The structure refinement reveals that this molecule displays the largest $\text{Sn}-\text{O}$ bond length for compounds including the $X=\text{O}\rightarrow\text{SnPh}_3\text{Cl}$ fragment ($X = \text{P}, \text{S}, \text{C}$, or V), 2.6644 (17) Å. However, an AIM topology analysis based on the wavefunction calculated from the refined X-ray structure shows the presence of a bond critical point (3, -1), lying on the interbasin surface separating the coordinated phosphate O atom and the Sn atom. This study thus shows that an actual polar covalent bond is formed between $(\text{PhO})_3\text{P}=\text{O}$ and SnPh_3Cl moieties.

1. Chemical context

An interesting feature of tin(IV) is its ability to perform as a hypervalent centre: pentacoordinated tin compounds, like chlorido(dimethyl sulfoxide)triphenyltin, $\text{SnPh}_3(\text{DMSO})\text{Cl}$ (Pouye *et al.*, 2018), are as common as tetracoordinated tin compounds, for example chloridotriphenyltin, SnPh_3Cl (Tse *et al.*, 1986; Ng, 1995). This leaves the possibility open to synthesize compounds with intermediate valency, between four and five. The title compound is such a compound, which is formally obtained as the adduct of SnPh_3Cl and triphenylphosphate, $(\text{PhO})_3\text{P}=\text{O}$, for which the X-ray structure is available (Svetich & Caughlan, 1965). While the phosphate group $\text{P}=\text{O}$ coordinates the Sn centre, more than four electrons in the valence shell of Sn, $4d^{10}5s^25p^2$, must be involved in the formation of the bonds around Sn. Herein, we are interested in the nature of the bond between Sn and the phosphate O atom.



2. Structural commentary

The title molecule, $\text{SnPh}_3\text{Cl}-(\text{PhO})_3\text{P}=\text{O}$, crystallizes in space group $P\bar{1}$ with one molecule in the asymmetric unit (Fig. 1). The $\text{P}=\text{O}$ group of the phosphate coordinates the Sn centre, *trans* to the Cl atom, with a $\text{P}-\text{O}-\text{Sn}$ angle of $177.58(12)^\circ$. The five-coordinate Sn centre displays a distorted trigonal-bipyramidal geometry, very different from the tetrahedral geometry observed for SnPh_3Cl , and consistent with dsp^3 hybrid orbitals on the metal centre. Conversely, the phosphate moiety in the title compound features a tetrahedral geometry close to that of free $(\text{PhO})_3\text{P}=\text{O}$. The main structural feature is the staggered arrangement of the six phenyl rings, minimizing intramolecular steric hindrance. The same conformation was previously obtained in the adduct between SnPh_3Cl and triphenylphosphine oxide $\text{Ph}_3\text{P}=\text{O}$ (Ng & Kumar Das, 1992) or in the complex chlorido[chloromethyl(diphenyl)phosphine oxide]triphenyltin, $\text{SnPh}_3\text{Cl}-\text{Ph}_2(\text{CH}_2\text{Cl})\text{P}=\text{O}$ (Kapoor *et al.*, 2007).

In the title compound, the $\text{Sn}-\text{O}$ bond length is $2.6644(17)$ Å. A survey of the CSD shows that for $X=\text{O}\rightarrow\text{SnPh}_3\text{Cl}$ fragments where $X = \text{P}, \text{S}, \text{C}$ or V , the $\text{X}=\text{O}-\text{Sn}$ angles range from 119.4 to 176.3° , while $\text{Sn}-\text{O}$ bond lengths range from 2.29 to 2.64 Å (CSD 5.43 with all updates; Groom *et al.*, 2016). There is no correlation between the bond lengths and angles ($R^2 = 0.002$ for a linear fit). The largest $\text{Sn}-\text{O}$ bond in the set of 40 structures retrieved from the CSD is 2.642 Å, for a dinuclear Sn complex (Gholivand *et al.*, 2015) closely related to the title compound. The title complex has thus the largest $\text{Sn}-\text{O}$ bond length and $\text{P}=\text{O}-\text{Sn}$ angle in this series, which could reflect a bond order less

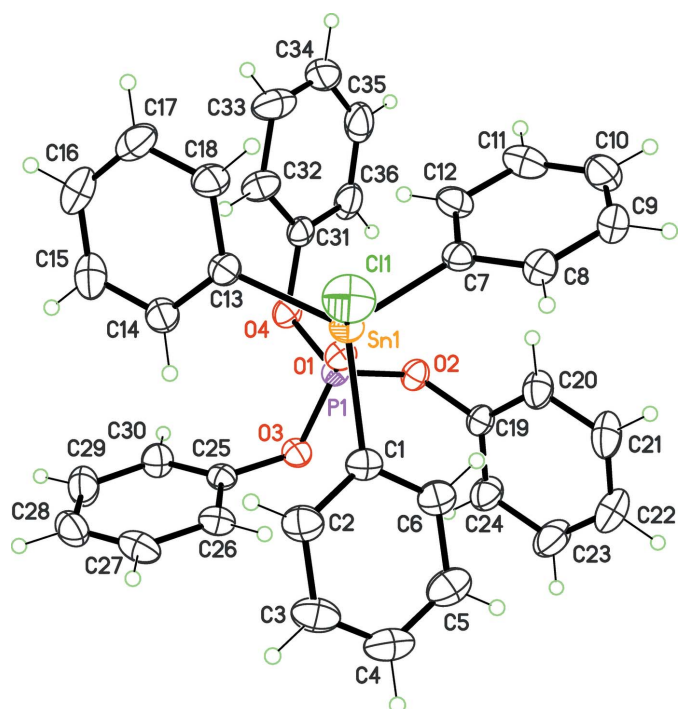


Figure 1

Molecular structure of the title compound viewed along the $\text{P}=\text{O}-\text{Sn}$ axis. Displacement ellipsoids for non-H atoms are drawn at the 30% probability level.

Table 1
Experimental details.

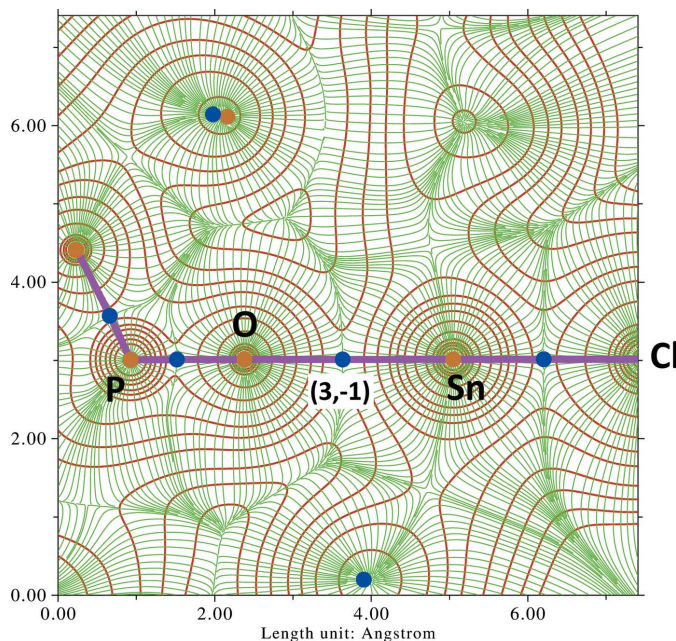
Crystal data	[$\text{Sn}(\text{C}_6\text{H}_5)_3\text{Cl}(\text{C}_{18}\text{H}_{15}\text{O}_4\text{P})$]
M_r	711.71
Crystal system, space group	Triclinic, $P\bar{1}$
Temperature (K)	295
a, b, c (Å)	$10.0455(4), 12.0370(5), 13.8304(6)$
α, β, γ (°)	$93.552(4), 93.469(3), 93.128(3)$
V (Å 3)	$1663.21(12)$
Z	2
Radiation type	Ag $K\alpha$, $\lambda = 0.56083$ Å
μ (mm $^{-1}$)	0.50
Crystal size (mm)	$0.40 \times 0.24 \times 0.16$
Data collection	
Diffractometer	Stoe Stadivari
Absorption correction	Multi-scan (<i>X-AREA</i> ; Stoe & Cie, 2018)
T_{\min}, T_{\max}	0.674, 1.000
No. of measured, independent and observed [$I > 2\sigma(I)$] reflections	49761, 9400, 6297
R_{int}	0.032
$(\sin \theta/\lambda)_{\text{max}}$ (Å $^{-1}$)	0.697
Refinement	
$R[F^2 > 2\sigma(F^2)], wR(F^2), S$	0.035, 0.097, 1.00
No. of reflections	9400
No. of parameters	388
H-atom treatment	H-atom parameters constrained
$\Delta\rho_{\text{max}}, \Delta\rho_{\text{min}}$ (e Å $^{-3}$)	0.76, -0.71

Computer programs: *X-AREA* (Stoe & Cie, 2018), *SHELXT2018/2* (Sheldrick, 2015a), *SHELXL2018/3* (Sheldrick, 2015b), *XP* in *SHELXTL-Plus* (Sheldrick, 2008) and *publCIF* (Westrip, 2010).

than 1 for the σ bond $\text{Sn}-\text{O}$. The situation is quite different, for example, for a non-hindered phosphastanninane, which forms dimers through $\text{P}=\text{O}-\text{Sn}$ bonds, with a short $\text{Sn}-\text{O}$ bond length of 2.425 Å (Weichmann & Meunier-Piret, 1993).

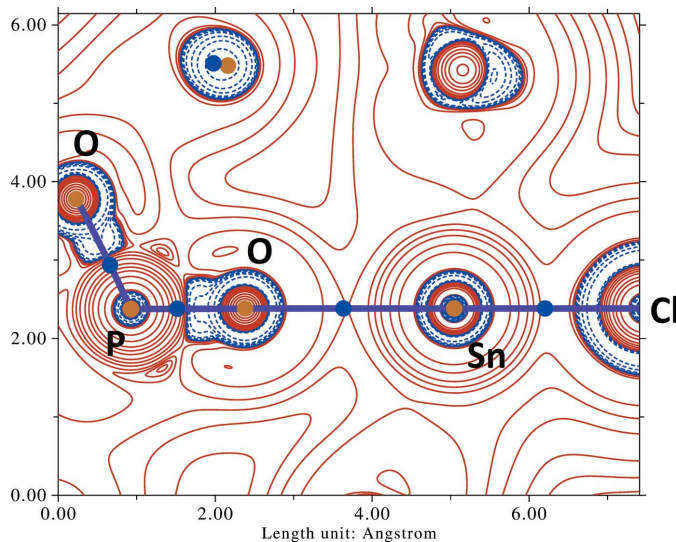
However, in the title compound, the SnPh_3Cl moiety is certainly bound to the phosphate, since the sum of van der Waals radii for Sn and O is 3.69 Å, much larger than the observed $\text{Sn}-\text{O}$ separation (Bondi, 1964). In other words, $\text{SnPh}_3\text{Cl}-(\text{PhO})_3\text{P}=\text{O}$ can not be described as a co-crystal between SnPh_3Cl and $(\text{PhO})_3\text{P}=\text{O}$. This can be confirmed through the topology analysis of electron density in the complex, and in particular the computation of critical points, in the context of the Bader's QTAIM theory (quantum theory of atoms in molecules; Bader, 2009). Therefore, starting from the *SHELXL* refinement (Table 1), a wave function was calculated using *ORCA* (Neese, 2018), and the structural model further refined with *olex2.refine* and *NoSphereA2* (Bourhis *et al.*, 2015; Kleemiss *et al.*, 2021) within *OLEX2* (Dolomanov *et al.*, 2009). The relativistic basis set x2c-SVP and the generalized gradient approximation PBE functional were used. This refined model included isotropic H atoms with free coordinates, and converged to $R_1 = 3.26\%$, a slight improvement over the *SHELXL* refinement at $R_1 = 3.48\%$.

A (3,-1) bond critical point is then observed at the midpoint of the atomic pair O1/Sn1, lying on the interbasin surface separating atoms O1 and Sn1 (Fig. 2). The charge density for this critical point is $\rho = 0.024$ a.u. (corresponding to 2.552×10^{10} C m $^{-3}$), and a topology bond path connects the

**Figure 2**

Contour map of the electron density ρ (brown contour lines) with the gradient vector field of ρ (green flux lines) in the vicinity of the $\text{P}=\text{O}-\text{Sn}-\text{Cl}$ group. Bond and nuclear critical points are represented by blue and brown dots, respectively, while the purple bold lines are the bond paths (Bader, 2009) connecting nuclear critical points. The map was calculated and plotted using *Multiwfn* (Lu & Chen, 2012).

nuclear critical points (3,-3) placed on O1 and Sn1. The nature of the Sn1—O1 bond can be further characterized by computing the Laplacian of the electron density, $\nabla^2(\rho)$, in the vicinity of the bond: in the valence-atomic orbital region

**Figure 3**

Contour map of the Laplacian of ρ in the vicinity of the $\text{P}=\text{O}-\text{Sn}-\text{Cl}$ group. Solid red lines are isocontours with positive Laplacian (charge depletion regions) and dashed blue lines are isocontours with negative Laplacian (charge accumulation regions). Bond critical points and nuclear critical points are shown as blue and brown dots, respectively. The purple bold lines are the bond paths (Bader, 2009) connecting nuclear critical points in the map. The map was calculated and plotted using *Multiwfn* (Lu & Chen, 2012).

Table 2
Hydrogen-bond geometry (\AA , $^\circ$).

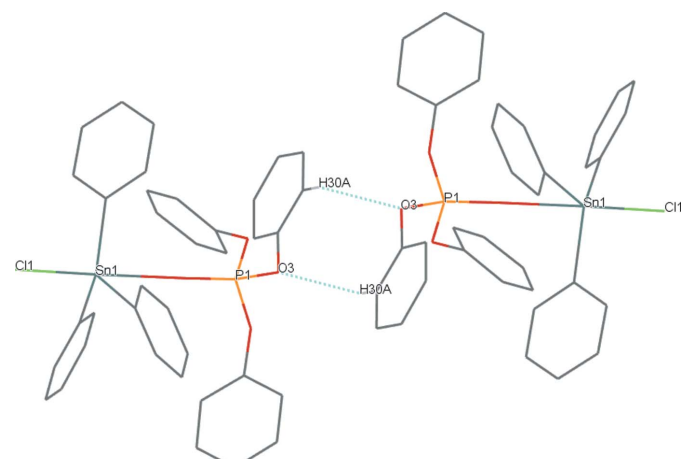
$D-\text{H}\cdots A$	$D-\text{H}$	$\text{H}\cdots A$	$D\cdots A$	$D-\text{H}\cdots A$
$\text{C30}-\text{H30A}\cdots \text{O3}^{\text{i}}$	0.93	2.71	3.526 (4)	147
$\text{C30}-\text{H30A}\cdots \text{O2}^{\text{i}}$	0.93	3.13	3.593 (4)	113

Symmetry code: (i) $-x + 1, -y + 1, -z + 2$.

between the O and Sn atoms, the bond critical point has a small critical density and a positive Laplacian (Fig. 3). Regions combining $\rho \rightarrow 0$ and $\nabla^2(\rho) > 0$ are dominated by closed-shell interactions suffering from Pauli repulsions, as in ionic bonds (for an extremely clear and well-written introduction to the valence-bond theory in the AIM context, see Shaik *et al.*, 2015). In the present case, the Sn1—O1 bond can thus be seen as a polar single σ (covalent) bond mainly characterized by electrostatic interactions. This description is obviously consistent with the large electronegativity gap between Sn and O, $\Delta\chi \approx 1.5$ on the Pauling scale. Moreover, the bond polarization is reflected in calculated CHELPG charges (atomic charges fitting the molecular electrostatic potential; Breneman & Wiberg, 1990): +0.597 for Sn1 and -0.543 for O1, as calculated by *Multiwfn* (Lu & Chen, 2012).

3. Supramolecular features

Although six phenyl rings are present in the molecular complex, its conformation does not favour the emergence of $\pi-\pi$ interactions in the crystal structure. The only relevant intermolecular interactions are weak C—H \cdots O contacts. Two neighbouring complexes are connected through weak interactions between the oxygen atoms O3 in the $(\text{PhO})_3\text{P}=\text{O}$ moieties, and the hydrogen atoms H30A belonging to neighbouring molecules ($d_{\text{H}\cdots \text{O}} = 2.71 \text{ \AA}$ and $\theta_{\text{C}-\text{H}\cdots \text{O}} = 146.8^\circ$; Table 2, entry 1). These interactions lead to discrete dimers, forming centrosymmetric $R_2^2(8)$ ring motifs (Fig. 4). Other similar contacts in the crystal have their C—H \cdots O angles below 120° (Table 2, entry 2), and are thus expected to have no contribution to crystal stabilization (Wood *et al.*, 2009).

**Figure 4**
Dimeric cluster in the crystal structure, formed through weak C—H \cdots O hydrogen bonds (dashed blue lines).

4. Synthesis and crystallization

This organotin complex was synthesized by reacting Ph_3PO_4 (1 mmol, 326 mg) on SnPh_3Cl (1 mmol, 385 mg) in ethanol. The mixture was refluxed ($T = 473$ K) under stirring for 1 h. The obtained solution was slightly cloudy, then it was filtered off. The filtrate was slowly evaporated at 300 K for one week, to give colourless crystals suitable for X-ray diffraction.

5. Refinement details

Crystal data, data collection and structure refinement details are summarized in Table 1. All H atoms were placed in calculated positions, with C—H bond lengths of 0.93 Å and $U_{\text{iso}}(\text{H}) = 1.2 U_{\text{eq}}$ (carrier C atom).

Acknowledgements

We thank Dr Hugo Vazquez-Lima (ICUAP, Puebla, Mexico) for guidance in the QTAIM interpretation.

Funding information

Funding for this research was provided by: Consejo Nacional de Ciencia y Tecnología (grant No. 268178).

References

- Bader, R. F. W. (2009). *J. Phys. Chem. A*, **113**, 10391–10396.
 Bondi, A. (1964). *J. Phys. Chem.* **68**, 441–451.
 Bourhis, L. J., Dolomanov, O. V., Gildea, R. J., Howard, J. A. K. & Puschmann, H. (2015). *Acta Cryst. A* **71**, 59–75.
 Breneman, C. M. & Wiberg, K. B. (1990). *J. Comput. Chem.* **11**, 361–373.
 Dolomanov, O. V., Bourhis, L. J., Gildea, R. J., Howard, J. A. K. & Puschmann, H. (2009). *J. Appl. Cryst.* **42**, 339–341.
 Gholivand, K., Gholami, A., Ebrahimi, A. A. V., Abolghasemi, S. T., Esrafil, M. D., Fadaei, F. T. & Schenk, K. J. (2015). *RSC Adv.* **5**, 17482–17492.
 Groom, C. R., Bruno, I. J., Lightfoot, M. P. & Ward, S. C. (2016). *Acta Cryst. B* **72**, 171–179.
 Kapoor, R. N., Cervantes-Lee, F. & Pannell, K. H. (2007). *J. Mex. Chem. Soc.* **51**, 122–128.
 Kleemiss, F., Dolomanov, O. V., Bodensteiner, M., Peyerimhoff, N., Midgley, L., Bourhis, L. J., Genoni, A., Malaspina, L. A., Jayatilaka, D., Spencer, J. L., White, F., Grundkötter-Stock, B., Steinhauer, S., Lentz, D., Puschmann, H. & Grabowsky, S. (2021). *Chem. Sci.* **12**, 1675–1692.
 Lu, T. & Chen, F. (2012). *J. Comput. Chem.* **33**, 580–592.
 Neese, F. (2018). *WIREs Comput. Mol. Sci.* **8**, e1327.
 Ng, S. W. (1995). *Acta Cryst. C* **51**, 2292–2293.
 Ng, S. W. & Kumar Das, V. G. (1992). *Acta Cryst. C* **48**, 1839–1841.
 Pouye, S. F., Cissé, I., Diop, L., Ríos-Merino, F. J. & Bernès, S. (2018). *Acta Cryst. E* **74**, 163–166.
 Shaik, S., Danovich, D., Braida, B., Wu, W. & Hiberty, P. C. (2015). *Struct. Bond.* **170**, 169–211. This book chapter is available from the HAL repository: <https://hal.archives-ouvertes.fr/hal-01627700>
 Sheldrick, G. M. (2008). *Acta Cryst. A* **64**, 112–122.
 Sheldrick, G. M. (2015a). *Acta Cryst. A* **71**, 3–8.
 Sheldrick, G. M. (2015b). *Acta Cryst. C* **71**, 3–8.
 Stoe & Cie (2018). *X-AREA* and *X-RED32*, Stoe & Cie, Darmstadt, Germany.
 Svetich, G. W. & Caughlan, C. N. (1965). *Acta Cryst.* **19**, 645–650.
 Tse, J. S., Lee, F. L. & Gabe, E. J. (1986). *Acta Cryst. C* **42**, 1876–1878.
 Weichmann, H. & Meunier-Piret, J. (1993). *Organometallics*, **12**, 4097–4103.
 Westrip, S. P. (2010). *J. Appl. Cryst.* **43**, 920–925.
 Wood, P. A., Allen, F. H. & Pidcock, E. (2009). *CrystEngComm*, **11**, 1563–1571.

supporting information

Acta Cryst. (2023). E79, 99–102 [https://doi.org/10.1107/S2056989023000270]

Synthesis and topology analysis of chloridotriphenyl(triphenyl phosphate- κO)tin(IV)

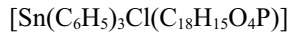
Serigne Fallou Pouye, Sylvain Bernès, Lamine Yaffa, Waly Diallo, Ibrahima Cissé, Cheikh Abdoul Khadir Diop, Mamadou Sidibé and Libasse Diop

Computing details

Data collection: *X-AREA* 1.86 (Stoe & Cie, 2018); cell refinement: *X-AREA* 1.86 (Stoe & Cie, 2018); data reduction: *X-AREA* 1.86 (Stoe & Cie, 2018); program(s) used to solve structure: *SHELXT2018/2* (Sheldrick, 2015a); program(s) used to refine structure: *SHELXL2018/3* (Sheldrick, 2015b); molecular graphics: *XP* in *SHELXTL-Plus* (Sheldrick, 2008); software used to prepare material for publication: *publCIF* (Westrip, 2010).

Chloridotriphenyl(triphenyl phosphate- κO)tin(IV)

Crystal data



$M_r = 711.71$

Triclinic, $P\bar{1}$

$a = 10.0455$ (4) Å

$b = 12.0370$ (5) Å

$c = 13.8304$ (6) Å

$\alpha = 93.552$ (4)°

$\beta = 93.469$ (3)°

$\gamma = 93.128$ (3)°

$V = 1663.21$ (12) Å³

$Z = 2$

$F(000) = 720$

$D_x = 1.421$ Mg m⁻³

Ag $K\alpha$ radiation, $\lambda = 0.56083$ Å

Cell parameters from 46721 reflections

$\theta = 2.3\text{--}25.3$ °

$\mu = 0.50$ mm⁻¹

$T = 295$ K

Prism, colourless

0.40 × 0.24 × 0.16 mm

Data collection

Stoe Stadivari

 diffractometer

Radiation source: Sealed X-ray tube, Axo Astix-
f Microfocus source

Graded multilayer mirror monochromator

Detector resolution: 5.81 pixels mm⁻¹

ω scans

Absorption correction: multi-scan
(X-AREA; Stoe & Cie, 2018)

$T_{\min} = 0.674$, $T_{\max} = 1.000$

49761 measured reflections

9400 independent reflections

6297 reflections with $I > 2\sigma(I)$

$R_{\text{int}} = 0.032$

$\theta_{\max} = 23.0$ °, $\theta_{\min} = 2.3$ °

$h = -12 \rightarrow 13$

$k = -16 \rightarrow 16$

$l = -19 \rightarrow 19$

Refinement

Refinement on F^2

388 parameters

Least-squares matrix: full

0 restraints

$R[F^2 > 2\sigma(F^2)] = 0.035$

0 constraints

$wR(F^2) = 0.097$

Primary atom site location: dual

$S = 1.00$

Secondary atom site location: difference Fourier

9400 reflections

map

Hydrogen site location: inferred from
neighbouring sites
H-atom parameters constrained

$$w = 1/[\sigma^2(F_o^2) + (0.0346P)^2 + 0.9327P]$$

$$\text{where } P = (F_o^2 + 2F_c^2)/3$$

$$(\Delta/\sigma)_{\max} = 0.001$$

$$\Delta\rho_{\max} = 0.76 \text{ e \AA}^{-3}$$

$$\Delta\rho_{\min} = -0.71 \text{ e \AA}^{-3}$$

Fractional atomic coordinates and isotropic or equivalent isotropic displacement parameters (\AA^2)

	<i>x</i>	<i>y</i>	<i>z</i>	$U_{\text{iso}}^*/U_{\text{eq}}$
Sn1	0.73207 (2)	0.23155 (2)	0.60158 (2)	0.06119 (8)
Cl1	0.79804 (12)	0.18751 (10)	0.43845 (7)	0.1046 (3)
C1	0.8729 (3)	0.3660 (2)	0.6418 (2)	0.0604 (7)
C2	0.8753 (4)	0.4636 (3)	0.5943 (3)	0.0792 (9)
H2A	0.814217	0.470870	0.542093	0.095*
C3	0.9677 (4)	0.5510 (3)	0.6234 (3)	0.0980 (12)
H3A	0.967353	0.616668	0.591253	0.118*
C4	1.0582 (4)	0.5410 (4)	0.6982 (4)	0.1008 (13)
H4A	1.120050	0.599718	0.717309	0.121*
C5	1.0591 (4)	0.4452 (4)	0.7457 (3)	0.1002 (12)
H5A	1.122164	0.438458	0.796706	0.120*
C6	0.9660 (3)	0.3576 (3)	0.7182 (2)	0.0774 (9)
H6A	0.966543	0.292768	0.751420	0.093*
C7	0.7760 (3)	0.0812 (2)	0.6660 (2)	0.0610 (7)
C8	0.8984 (3)	0.0358 (3)	0.6565 (3)	0.0816 (9)
H8A	0.961034	0.069823	0.619299	0.098*
C9	0.9288 (4)	-0.0604 (4)	0.7022 (4)	0.1027 (14)
H9A	1.011318	-0.090327	0.695210	0.123*
C10	0.8386 (5)	-0.1106 (3)	0.7568 (4)	0.1053 (14)
H10A	0.860158	-0.173904	0.788342	0.126*
C11	0.7168 (5)	-0.0686 (3)	0.7656 (3)	0.0940 (11)
H11A	0.654337	-0.104370	0.801756	0.113*
C12	0.6851 (3)	0.0271 (3)	0.7210 (2)	0.0733 (8)
H12A	0.601730	0.055436	0.728065	0.088*
C13	0.5272 (3)	0.2577 (2)	0.56897 (19)	0.0601 (6)
C14	0.4720 (3)	0.3564 (3)	0.5952 (2)	0.0714 (8)
H14A	0.526938	0.416259	0.622712	0.086*
C15	0.3369 (4)	0.3680 (4)	0.5813 (3)	0.0947 (12)
H15A	0.301226	0.435244	0.599491	0.114*
C16	0.2548 (4)	0.2808 (5)	0.5407 (3)	0.1001 (13)
H16A	0.163297	0.288594	0.532147	0.120*
C17	0.3069 (4)	0.1832 (4)	0.5131 (3)	0.0960 (12)
H17A	0.250940	0.124019	0.485647	0.115*
C18	0.4433 (3)	0.1712 (3)	0.5257 (2)	0.0771 (9)
H18A	0.478618	0.104607	0.504898	0.093*
P1	0.61706 (6)	0.31982 (6)	0.87530 (5)	0.04891 (15)
O1	0.65797 (17)	0.28553 (15)	0.77937 (12)	0.0551 (4)
O2	0.69211 (17)	0.26752 (17)	0.96296 (13)	0.0599 (4)
O3	0.63487 (19)	0.44813 (15)	0.90462 (13)	0.0581 (4)
O4	0.46665 (17)	0.29271 (16)	0.89412 (14)	0.0599 (5)

C19	0.8332 (3)	0.2685 (2)	0.97307 (19)	0.0580 (6)
C20	0.8990 (3)	0.1840 (3)	0.9319 (2)	0.0817 (10)
H20A	0.852379	0.127052	0.893273	0.098*
C21	1.0357 (4)	0.1836 (4)	0.9480 (3)	0.1044 (14)
H21A	1.081703	0.124937	0.922090	0.125*
C22	1.1033 (4)	0.2699 (5)	1.0023 (3)	0.1053 (14)
H22A	1.195691	0.270597	1.012357	0.126*
C23	1.0363 (4)	0.3540 (4)	1.0413 (3)	0.1084 (14)
H23A	1.083077	0.412464	1.078131	0.130*
C24	0.8999 (3)	0.3543 (3)	1.0273 (3)	0.0854 (10)
H24A	0.853900	0.412281	1.054415	0.102*
C25	0.5859 (3)	0.5270 (2)	0.84188 (18)	0.0531 (6)
C26	0.6648 (3)	0.5650 (2)	0.7723 (2)	0.0670 (7)
H26A	0.749342	0.538655	0.765506	0.080*
C27	0.6166 (4)	0.6431 (3)	0.7122 (3)	0.0854 (10)
H27A	0.668221	0.668757	0.663711	0.103*
C28	0.4931 (5)	0.6831 (3)	0.7239 (3)	0.0926 (12)
H28A	0.460557	0.735260	0.683014	0.111*
C29	0.4173 (4)	0.6455 (3)	0.7964 (3)	0.0966 (12)
H29A	0.334446	0.674085	0.805287	0.116*
C30	0.4631 (3)	0.5663 (3)	0.8557 (2)	0.0732 (8)
H30A	0.411566	0.540112	0.904119	0.088*
C31	0.4067 (2)	0.1843 (2)	0.8716 (2)	0.0599 (7)
C32	0.3518 (3)	0.1565 (3)	0.7802 (3)	0.0808 (9)
H32A	0.355169	0.207309	0.732295	0.097*
C33	0.2910 (4)	0.0513 (4)	0.7604 (4)	0.1065 (14)
H33A	0.254556	0.030130	0.698124	0.128*
C34	0.2843 (4)	-0.0213 (4)	0.8311 (5)	0.126 (2)
H34A	0.243098	-0.091981	0.817172	0.151*
C35	0.3373 (4)	0.0085 (4)	0.9224 (5)	0.133 (2)
H35A	0.331360	-0.041837	0.970579	0.159*
C36	0.4003 (3)	0.1133 (3)	0.9443 (3)	0.0913 (12)
H36A	0.436863	0.134381	1.006540	0.110*

Atomic displacement parameters (\AA^2)

	U^{11}	U^{22}	U^{33}	U^{12}	U^{13}	U^{23}
Sn1	0.06419 (12)	0.06082 (13)	0.05806 (12)	0.00085 (9)	0.00682 (8)	-0.00058 (8)
C11	0.1275 (8)	0.1191 (8)	0.0673 (5)	0.0055 (7)	0.0309 (5)	-0.0156 (5)
C1	0.0594 (15)	0.0638 (17)	0.0582 (16)	-0.0030 (13)	0.0183 (12)	-0.0024 (13)
C2	0.084 (2)	0.083 (2)	0.072 (2)	-0.0097 (18)	0.0163 (17)	0.0134 (17)
C3	0.107 (3)	0.084 (3)	0.105 (3)	-0.025 (2)	0.030 (2)	0.017 (2)
C4	0.091 (3)	0.095 (3)	0.112 (3)	-0.033 (2)	0.024 (2)	-0.016 (3)
C5	0.086 (2)	0.116 (3)	0.092 (3)	-0.014 (2)	-0.009 (2)	-0.014 (2)
C6	0.0771 (19)	0.078 (2)	0.075 (2)	-0.0028 (17)	0.0031 (16)	-0.0006 (17)
C7	0.0608 (15)	0.0557 (16)	0.0642 (17)	0.0002 (12)	0.0015 (13)	-0.0097 (13)
C8	0.0617 (17)	0.077 (2)	0.105 (3)	0.0056 (16)	-0.0001 (17)	-0.0011 (19)
C9	0.076 (2)	0.085 (3)	0.144 (4)	0.019 (2)	-0.029 (2)	0.000 (3)

C10	0.124 (4)	0.067 (2)	0.121 (4)	0.008 (2)	-0.030 (3)	0.011 (2)
C11	0.129 (3)	0.065 (2)	0.087 (3)	-0.014 (2)	0.016 (2)	0.0034 (18)
C12	0.082 (2)	0.0543 (17)	0.083 (2)	0.0007 (15)	0.0145 (17)	-0.0064 (15)
C13	0.0697 (16)	0.0635 (17)	0.0458 (14)	0.0025 (13)	-0.0029 (12)	0.0015 (12)
C14	0.084 (2)	0.0667 (19)	0.0622 (18)	0.0093 (16)	-0.0065 (15)	-0.0029 (14)
C15	0.099 (3)	0.108 (3)	0.080 (2)	0.043 (2)	-0.003 (2)	0.005 (2)
C16	0.070 (2)	0.153 (4)	0.078 (2)	0.017 (3)	-0.0119 (18)	0.016 (3)
C17	0.082 (2)	0.120 (3)	0.080 (2)	-0.022 (2)	-0.0217 (19)	0.008 (2)
C18	0.089 (2)	0.071 (2)	0.0669 (19)	-0.0022 (17)	-0.0087 (16)	-0.0092 (16)
P1	0.0494 (3)	0.0549 (4)	0.0420 (3)	0.0027 (3)	0.0035 (3)	-0.0006 (3)
O1	0.0571 (9)	0.0637 (11)	0.0437 (9)	0.0015 (8)	0.0061 (7)	-0.0044 (8)
O2	0.0549 (10)	0.0743 (13)	0.0510 (10)	0.0046 (9)	0.0009 (8)	0.0111 (9)
O3	0.0720 (11)	0.0541 (10)	0.0464 (9)	0.0041 (9)	-0.0033 (8)	-0.0042 (8)
O4	0.0513 (9)	0.0674 (12)	0.0615 (11)	0.0064 (9)	0.0094 (8)	0.0008 (9)
C19	0.0562 (14)	0.0694 (18)	0.0484 (14)	0.0061 (13)	-0.0022 (11)	0.0069 (12)
C20	0.080 (2)	0.093 (2)	0.070 (2)	0.0265 (18)	-0.0112 (16)	-0.0145 (18)
C21	0.088 (3)	0.128 (4)	0.100 (3)	0.053 (3)	0.000 (2)	-0.005 (3)
C22	0.063 (2)	0.155 (4)	0.097 (3)	0.016 (2)	-0.011 (2)	0.005 (3)
C23	0.073 (2)	0.128 (4)	0.117 (3)	-0.002 (2)	-0.020 (2)	-0.019 (3)
C24	0.074 (2)	0.091 (2)	0.087 (2)	0.0094 (18)	-0.0114 (18)	-0.0196 (19)
C25	0.0626 (14)	0.0483 (14)	0.0464 (13)	-0.0016 (11)	0.0005 (11)	-0.0056 (11)
C26	0.0746 (18)	0.0590 (17)	0.0669 (18)	-0.0069 (14)	0.0164 (14)	-0.0012 (14)
C27	0.126 (3)	0.0600 (19)	0.070 (2)	-0.012 (2)	0.015 (2)	0.0070 (16)
C28	0.126 (3)	0.066 (2)	0.083 (3)	0.004 (2)	-0.022 (2)	0.0166 (18)
C29	0.085 (2)	0.096 (3)	0.112 (3)	0.028 (2)	-0.001 (2)	0.018 (2)
C30	0.0692 (18)	0.081 (2)	0.071 (2)	0.0089 (16)	0.0116 (15)	0.0089 (16)
C31	0.0414 (12)	0.0672 (17)	0.0730 (18)	0.0040 (12)	0.0091 (12)	0.0137 (14)
C32	0.0707 (19)	0.091 (2)	0.078 (2)	-0.0193 (17)	0.0099 (16)	0.0018 (18)
C33	0.078 (2)	0.108 (3)	0.127 (4)	-0.028 (2)	0.010 (2)	-0.022 (3)
C34	0.069 (2)	0.075 (3)	0.232 (7)	-0.010 (2)	-0.009 (3)	0.016 (4)
C35	0.071 (2)	0.109 (4)	0.224 (6)	-0.005 (2)	-0.017 (3)	0.096 (4)
C36	0.0629 (18)	0.107 (3)	0.107 (3)	0.0014 (18)	-0.0116 (18)	0.050 (2)

Geometric parameters (\AA , $^\circ$)

Sn1—C1	2.116 (3)	P1—O4	1.5690 (18)
Sn1—C7	2.122 (3)	P1—O3	1.5701 (19)
Sn1—C13	2.124 (3)	P1—O2	1.5718 (19)
Sn1—Cl1	2.4252 (9)	O2—C19	1.415 (3)
Sn1—O1	2.6644 (17)	O3—C25	1.414 (3)
C1—C6	1.380 (4)	O4—C31	1.416 (3)
C1—C2	1.381 (4)	C19—C20	1.357 (4)
C2—C3	1.388 (5)	C19—C24	1.359 (4)
C2—H2A	0.9300	C20—C21	1.378 (5)
C3—C4	1.351 (6)	C20—H20A	0.9300
C3—H3A	0.9300	C21—C22	1.367 (6)
C4—C5	1.362 (6)	C21—H21A	0.9300
C4—H4A	0.9300	C22—C23	1.349 (6)

C5—C6	1.389 (5)	C22—H22A	0.9300
C5—H5A	0.9300	C23—C24	1.373 (5)
C6—H6A	0.9300	C23—H23A	0.9300
C7—C8	1.382 (4)	C24—H24A	0.9300
C7—C12	1.385 (4)	C25—C30	1.365 (4)
C8—C9	1.393 (5)	C25—C26	1.368 (4)
C8—H8A	0.9300	C26—C27	1.381 (5)
C9—C10	1.355 (6)	C26—H26A	0.9300
C9—H9A	0.9300	C27—C28	1.369 (6)
C10—C11	1.359 (6)	C27—H27A	0.9300
C10—H10A	0.9300	C28—C29	1.379 (6)
C11—C12	1.382 (5)	C28—H28A	0.9300
C11—H11A	0.9300	C29—C30	1.377 (5)
C12—H12A	0.9300	C29—H29A	0.9300
C13—C14	1.376 (4)	C30—H30A	0.9300
C13—C18	1.386 (4)	C31—C36	1.362 (4)
C14—C15	1.375 (5)	C31—C32	1.362 (4)
C14—H14A	0.9300	C32—C33	1.380 (5)
C15—C16	1.368 (6)	C32—H32A	0.9300
C15—H15A	0.9300	C33—C34	1.354 (7)
C16—C17	1.355 (6)	C33—H33A	0.9300
C16—H16A	0.9300	C34—C35	1.359 (7)
C17—C18	1.387 (5)	C34—H34A	0.9300
C17—H17A	0.9300	C35—C36	1.388 (6)
C18—H18A	0.9300	C35—H35A	0.9300
P1—O1	1.4547 (18)	C36—H36A	0.9300
C1—Sn1—C7	114.01 (11)	O4—P1—O3	102.20 (11)
C1—Sn1—C13	121.56 (11)	O1—P1—O2	115.88 (11)
C7—Sn1—C13	116.86 (11)	O4—P1—O2	102.24 (10)
C1—Sn1—Cl1	98.73 (8)	O3—P1—O2	102.52 (10)
C7—Sn1—Cl1	99.82 (8)	P1—O1—Sn1	177.58 (12)
C13—Sn1—Cl1	99.13 (8)	C19—O2—P1	121.84 (16)
C6—C1—C2	118.1 (3)	C25—O3—P1	120.89 (15)
C6—C1—Sn1	119.7 (2)	C31—O4—P1	120.63 (16)
C2—C1—Sn1	122.2 (2)	C20—C19—C24	121.3 (3)
C1—C2—C3	120.8 (4)	C20—C19—O2	120.6 (3)
C1—C2—H2A	119.6	C24—C19—O2	118.1 (3)
C3—C2—H2A	119.6	C19—C20—C21	119.3 (4)
C4—C3—C2	120.2 (4)	C19—C20—H20A	120.3
C4—C3—H3A	119.9	C21—C20—H20A	120.3
C2—C3—H3A	119.9	C22—C21—C20	119.6 (4)
C3—C4—C5	120.2 (4)	C22—C21—H21A	120.2
C3—C4—H4A	119.9	C20—C21—H21A	120.2
C5—C4—H4A	119.9	C23—C22—C21	120.2 (4)
C4—C5—C6	120.2 (4)	C23—C22—H22A	119.9
C4—C5—H5A	119.9	C21—C22—H22A	119.9
C6—C5—H5A	119.9	C22—C23—C24	120.7 (4)

C1—C6—C5	120.5 (4)	C22—C23—H23A	119.7
C1—C6—H6A	119.8	C24—C23—H23A	119.7
C5—C6—H6A	119.8	C19—C24—C23	118.9 (4)
C8—C7—C12	117.8 (3)	C19—C24—H24A	120.6
C8—C7—Sn1	120.8 (2)	C23—C24—H24A	120.6
C12—C7—Sn1	121.4 (2)	C30—C25—C26	122.2 (3)
C7—C8—C9	120.6 (4)	C30—C25—O3	118.5 (2)
C7—C8—H8A	119.7	C26—C25—O3	119.2 (3)
C9—C8—H8A	119.7	C25—C26—C27	118.7 (3)
C10—C9—C8	120.3 (4)	C25—C26—H26A	120.7
C10—C9—H9A	119.8	C27—C26—H26A	120.7
C8—C9—H9A	119.8	C28—C27—C26	120.3 (3)
C9—C10—C11	120.0 (4)	C28—C27—H27A	119.8
C9—C10—H10A	120.0	C26—C27—H27A	119.8
C11—C10—H10A	120.0	C27—C28—C29	119.7 (3)
C10—C11—C12	120.4 (4)	C27—C28—H28A	120.2
C10—C11—H11A	119.8	C29—C28—H28A	120.2
C12—C11—H11A	119.8	C30—C29—C28	120.7 (4)
C11—C12—C7	120.8 (3)	C30—C29—H29A	119.7
C11—C12—H12A	119.6	C28—C29—H29A	119.7
C7—C12—H12A	119.6	C25—C30—C29	118.4 (3)
C14—C13—C18	118.1 (3)	C25—C30—H30A	120.8
C14—C13—Sn1	122.1 (2)	C29—C30—H30A	120.8
C18—C13—Sn1	119.7 (2)	C36—C31—C32	122.4 (3)
C15—C14—C13	121.0 (3)	C36—C31—O4	118.1 (3)
C15—C14—H14A	119.5	C32—C31—O4	119.4 (3)
C13—C14—H14A	119.5	C31—C32—C33	118.5 (4)
C16—C15—C14	120.2 (4)	C31—C32—H32A	120.8
C16—C15—H15A	119.9	C33—C32—H32A	120.8
C14—C15—H15A	119.9	C34—C33—C32	120.3 (4)
C17—C16—C15	119.9 (4)	C34—C33—H33A	119.9
C17—C16—H16A	120.0	C32—C33—H33A	119.9
C15—C16—H16A	120.0	C33—C34—C35	120.5 (4)
C16—C17—C18	120.3 (4)	C33—C34—H34A	119.7
C16—C17—H17A	119.8	C35—C34—H34A	119.7
C18—C17—H17A	119.8	C34—C35—C36	120.5 (4)
C13—C18—C17	120.4 (4)	C34—C35—H35A	119.7
C13—C18—H18A	119.8	C36—C35—H35A	119.7
C17—C18—H18A	119.8	C31—C36—C35	117.7 (4)
O1—P1—O4	116.16 (11)	C31—C36—H36A	121.1
O1—P1—O3	115.72 (11)	C35—C36—H36A	121.1
C6—C1—C2—C3	-0.8 (5)	O2—P1—O4—C31	-77.4 (2)
Sn1—C1—C2—C3	179.0 (3)	P1—O2—C19—C20	-89.0 (3)
C1—C2—C3—C4	0.9 (6)	P1—O2—C19—C24	92.9 (3)
C2—C3—C4—C5	-0.2 (7)	C24—C19—C20—C21	2.1 (5)
C3—C4—C5—C6	-0.7 (7)	O2—C19—C20—C21	-176.0 (3)
C2—C1—C6—C5	0.0 (5)	C19—C20—C21—C22	-2.2 (6)

Sn1—C1—C6—C5	−179.9 (3)	C20—C21—C22—C23	1.2 (7)
C4—C5—C6—C1	0.8 (6)	C21—C22—C23—C24	0.0 (8)
C12—C7—C8—C9	−0.8 (5)	C20—C19—C24—C23	−0.9 (6)
Sn1—C7—C8—C9	177.4 (3)	O2—C19—C24—C23	177.2 (3)
C7—C8—C9—C10	−0.2 (6)	C22—C23—C24—C19	−0.2 (7)
C8—C9—C10—C11	1.4 (7)	P1—O3—C25—C30	95.6 (3)
C9—C10—C11—C12	−1.6 (7)	P1—O3—C25—C26	−87.1 (3)
C10—C11—C12—C7	0.6 (6)	C30—C25—C26—C27	−2.0 (4)
C8—C7—C12—C11	0.6 (5)	O3—C25—C26—C27	−179.2 (3)
Sn1—C7—C12—C11	−177.6 (3)	C25—C26—C27—C28	1.3 (5)
C18—C13—C14—C15	1.7 (5)	C26—C27—C28—C29	0.5 (6)
Sn1—C13—C14—C15	−174.0 (3)	C27—C28—C29—C30	−1.6 (6)
C13—C14—C15—C16	−0.1 (6)	C26—C25—C30—C29	0.9 (5)
C14—C15—C16—C17	−0.8 (6)	O3—C25—C30—C29	178.1 (3)
C15—C16—C17—C18	−0.1 (6)	C28—C29—C30—C25	0.9 (6)
C14—C13—C18—C17	−2.6 (5)	P1—O4—C31—C36	96.4 (3)
Sn1—C13—C18—C17	173.3 (3)	P1—O4—C31—C32	−86.9 (3)
C16—C17—C18—C13	1.8 (6)	C36—C31—C32—C33	−2.0 (5)
O1—P1—O2—C19	49.9 (2)	O4—C31—C32—C33	−178.5 (3)
O4—P1—O2—C19	177.3 (2)	C31—C32—C33—C34	1.3 (6)
O3—P1—O2—C19	−77.1 (2)	C32—C33—C34—C35	−0.1 (7)
O1—P1—O3—C25	50.1 (2)	C33—C34—C35—C36	−0.6 (8)
O4—P1—O3—C25	−77.1 (2)	C32—C31—C36—C35	1.3 (5)
O2—P1—O3—C25	177.17 (18)	O4—C31—C36—C35	177.8 (3)
O1—P1—O4—C31	49.7 (2)	C34—C35—C36—C31	0.0 (7)
O3—P1—O4—C31	176.67 (19)		

Hydrogen-bond geometry (Å, °)

D—H···A	D—H	H···A	D···A	D—H···A
C30—H30A···O3 ⁱ	0.93	2.71	3.526 (4)	147
C30—H30A···O2 ⁱ	0.93	3.13	3.593 (4)	113

Symmetry code: (i) $-x+1, -y+1, -z+2$.